Artifact and noise stripping on low-field brain MRI

Nur Faiza Ishak, Rajasvaran Logeswaran, Wooi-Haw Tan

***Abstract*—**Low-field Magnetic Resonance Imaging (MRI) is a relatively new technology that is used in operating rooms to allow real-time imaging. The images produced are valuable for guidance and assessment during the surgery, but the low signal strength produces very low resolution images with noise and artifacts. This study shows that implementation of a dynamic pre-processing algorithm to extract the brain region in low-field MRI images is crucial in order to accurately segment the brain image. Conceptually, histogram-based analysis indicates that most low-field MR images consist of three peaks, where the first and second peaks summarize the background and artifacts, respectively, while the third peak is the region-of-interest (ROI). This paper provides some useful insight of steps that could be taken prior to brain segmentation. Promising results are reported for both qualitative and quantitative measurements.

***Keywords*—** Dynamic thresholding, Histogram analysis, Image enhancement, Magnetic Resonance Imaging (MRI), Normalization.

I. Introduction

IMAGE processing techniques make it possible to extract meaningful information from medical images. Brain Magnetic Resonance Imaging (MRI) images provide information of brain parts such as white matter (WM), gray matter (GM), cerebrospinal fluid (CSF), ventricles, skull and injuries such as bleeding, cyst, tumor and skull fracture. Low-field MRI is vital for sensitive surgery to allow real-time imaging in the operation theatre. An open low-field system would have a number of advantages over its conventional counterpart, including low-cost, reduced MR compatibility demands on instruments to minimize distortion, reduced fringe fields and the relative ease of movement and usage. The main problem with low-field MRI is its low resolution images. To achieve the best result in diagnosing disease, medical images must have good quality and be free from noise and artifacts.

Manuscript received January 9, 2009: This work was supported in part by the Ministry of Science, Technology and Innovation (MOSTI), Malaysia under the science fund grant.

N. Faiza Ishak is a Research Officer with the Faculty of Engineering, Multimedia University, 63100 Cyberjaya, Selangor, Malaysia (Phone: +603-8312-5258; fax: +603-8318-3029; e-mail: nur.faiza@mmu.edu.my).

R. Logeswaran is a Senior Lecturer with the Faculty of Engineering, Multimedia University, 63100 Cyberjaya, Selangor, Malaysia (e-mail: loges@ieee.org).

W.H. Tan is a lecturer with the Faculty of Engineering, Multimedia University, 63100 Cyberjaya, Selangor, Malaysia (e-mail: twhaw@mmu.edu.my).

Brain stripping is used to classify head image elements into two rigid classes, brain and non-brain [1]. It should be noted that a simple segmentation scheme used on conventional MRI images is a priori not sufficient to solve the problem. In additional, Gribkov [2] proposed a few segmentation methods on low contrast images and segmentation of domains with varying intensity. Fig. 1 shows the flowchart for typical brain segmentation which consists of 5 steps [3].

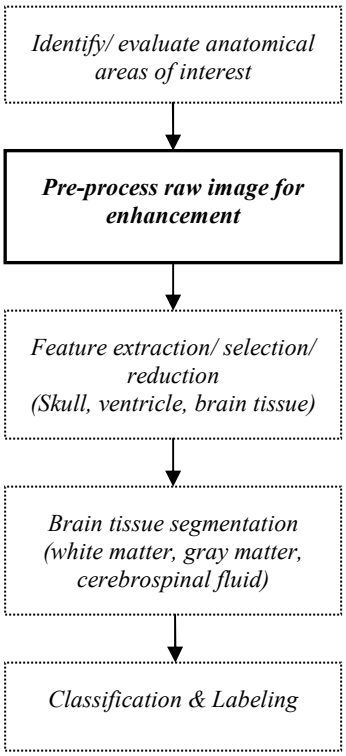

Fig. 1. Flowchart of complete brain segmentation on low-field MRI brain

The first step is to identify anatomical areas of interest in order to diagnose diseases and injuries. Usually this is done by the medical experts or radiologist in the hospital. Pre-processing techniques will be applied next for image enhancement. Since low-field brain MRI produces low resolution images, this step is crucial in making the region-of-interest (ROI) to appear clearer and noise-free. Once the pre-processing step is completed, feature extraction will be applied

to efficiently specify the boundaries between the brain structures to be identified, e.g. skull, brain tissues as well as ventricles. Segmentation will be used to distinguish the regions corresponding to different tissue types. Finally, the segmented regions will be labeled accordingly.

This paper proposes a complete pre-processing module using dynamic thresholding. There has been a lot of research work on pre-processing techniques [4], image intensity analysis [5-8] and image normalization [9-11] for conventional MR images. However, most of the techniques proposed are not directly applicable to low-field MR images [12]. Hence, an improved method of pre-processing low-field MR images is required. The technique should allow the structure of the brain to be more visible in the low-field MRI images.

In the pre-processing phase, normalization and background removal will be able to reduce the distortion of gray level and contrast [13]. A typical pre-processing phase usually consists of smoothing, edge detection, binarization, noise filtering as well as image sharpening [14-15]. These techniques are applicable to medical images as well as common images. Besides, effective image enhancement for medical diagnosis should consider the basic human visual properties for more efficient diagnosis.

The structure of this paper is as follows. The next section briefly discusses the background of low-field MRI. Section 3 describes the proposed histogram analysis method for low-field MRI images. The performance assessment is given in Section 4, which is followed by the conclusion in Section 5.

II. Background

What advantages of low-field MRI make it more suitable for brain surgery? The much simpler magnet setup offers many advantages: the possibility of using open magnets (minimizes claustrophobia), less static magnetic field exposure to the surrounding area, less costly equipment that is well-suited for the standard operating room (OR) environment, compatible with the electronic equipment and surgical tools, and relatively small size that is practical in cramped spaces. Furthermore, in situations where high-field strengths may drown out subtle signal differences, the low-field MRI becomes invaluable to detect these (such as in differentiating cancerous and non-cancerous tissue [16]).

It is usable in the OR and hence can update images to reflect the changes in anatomy after opening the skull in neurosurgery [17]. Furthermore, open low-field MRI is preferable to the tunnel-style conventional MRI for claustrophobic patients. Several previous studies have compared conventional MRI (1.5T) versus low-field MRI (0.15T), with most indicating no significant clinical differences in interpretations of low-field versus conventional images [18]. Thus, they are clinically applicable in operations and even routine checkups.

However, since low-field MRI uses low strength electromagnetic fields, noisy low resolution images are produced. In contrast, high-field MRI machines (approximately 7T) are able to produce clear detailed images with almost no noise at all. Considering the above, the motivation to enhance the low-field images is so that the same conventional and high-field MRI processing techniques and applications could be applied to the pre-processed low-field MRI images, allowing it to capitalize on the existing findings and advances technology.

Histogram analysis has been widely used in medical image processing. Background rejection is one of the common methods based on histogram analysis, where approximately 10% of the maximum gray level is eliminated [19]. However, since the intensity non-uniformity may exist in all directions, usually the normalization procedure will be repeated for all directions. Identifying optimal thresholds is always a challenge in MRI due to the wide variance in inter-patient and inter-image intensity distributions.

Fig. 2 shows the differences in conventional and low-field MRI images. Both images were taken from the same patient, for the same slice of the brain. However, the quality is noticeably worse in the low-field brain image. Not only is the noise level increased, but the orientation and coverage of the brain is affected as well due to the small aperture of the low-field machine. The lower part of the brain is no longer visible and an artifact is present at the top left (although not very visible in this image, it hinders automatic processing).

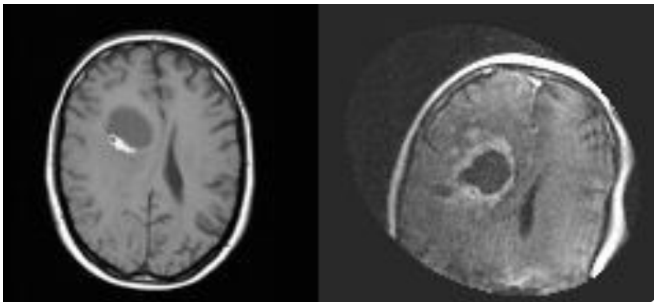

Fig. 2. Conventional MRI (left) and low-field MRI (right) images

Low-field MRI usually has a gray or black background with an elliptic artifact. The background should be removed as it is not part of the brain. This technique has been used in [20] as one of the pre-processing steps in brain region extraction. In [19], it was expected that a distinct peak in the histogram exist for determining the threshold value for the entire image, such that the image could be properly enhanced. Furthermore, this technique aims at disconnecting, as much as possible, the brain from surrounding structures. For instance, the low intensity eliminates the ventricle while the high intensity will eliminate the skull. However, this adaptation is difficult to perform automatically due to the large inter-image contrast variety.

III. Histogram Analysis

As low-field MRI equipment is still quite rare, a database of only 14 patients was available in this work. Each 128x128

pixels image was analyzed in terms of its intensity histogram. The parts of interest in a typical low-field MRI brain image are labeled in Fig. 3(a), with its histogram given in Fig. 3(b). Any pre-processing undertaken should preserve all the ROI, which in this case are the labeled areas excluding the artifact and background.

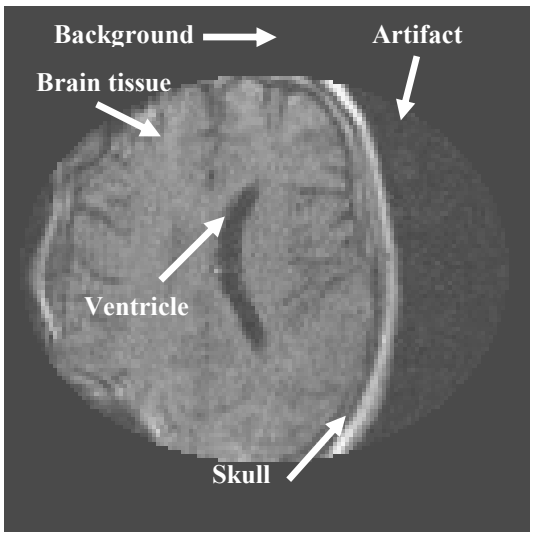

(a) Original image

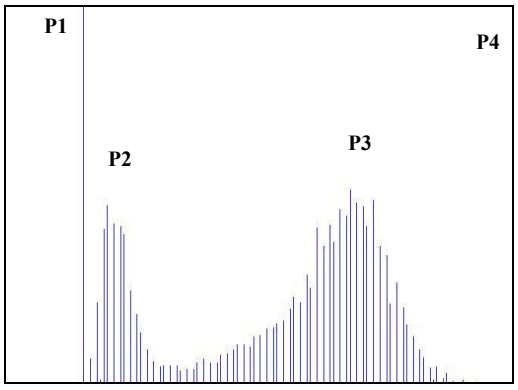

(b) Histogram

Fig. 3. Low-field MRI brain image and histogram

Upon inspection of the histogram, it is found that three peaks exist. P1, the first peak, is expected to be the background of the image, while P2 may contain most of the unwanted artifacts. As such, the object of interest, which is the brain, should be represented by P3. The fourth peak (P4) exists at intensity 255 in most images. It is present in Fig. 5(b), although not obvious. P4, being the highest intensity, is expected to be parts of the skull and bleeding in the brain.

The objective of image processing of the MRI brain is to extract the features, more specifically the brain tissue, ventricle, skull, diseased brain areas and abnormalities. Fig. 4 shows the detailed proposed method for pre-processing the image. Three main steps are to be taken, namely, background elimination, artifact elimination and finally image normalization. Elimination of undesirable regions is crucial in order to obtain precise segmentation of the brain.

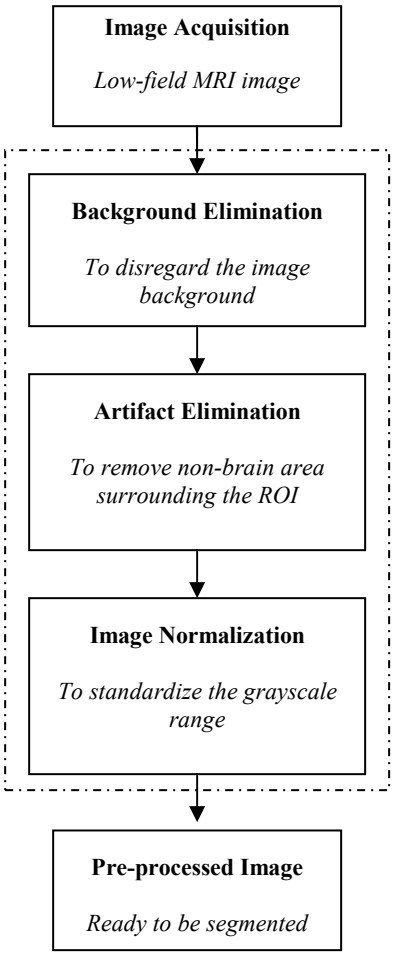

Fig. 4. Flowchart of image pre-processing module

A. Histogram Truncation

To examine the above hypothesis, histogram-based pre-processing techniques were applied to the image database. The image was then normalized to enhance its contrast. Normalization is crucial for the extraction and segmentation of the ROI for future work. This reduces the dynamic range of intensities between images, standardizing them and making them more suitable for subsequent processing.

The process initiates with the elimination of the first peak (P1), which is expected to be the background. By referring to the result (Fig. 5(b)) of the sample image in Fig. 5(a), it is shown that the background of the image is removed once the P1 has been eliminated. The remaining region is the elliptical shaped brain with the artifact. This supports the assumption that the first peak consists mostly of the background and its truncation eliminates the uncounted image background.

The next step is artifact elimination, i.e. the second peak (P2). By determining the maximum intensity of P2, (1) is used to choose the intensity range in the elimination technique.

$$\text{Threshold, } T = \frac{\max(\text{P2}) - \min(P1)}{p} \quad (1)$$

where max(P2) is the maximum intensity value of P2, min*(P1)* is minimum intensity of the P1 truncated image *(P1),* and *p* is the fraction of the slope for each thresholding step.

Very small steps (e.g *p*=1/5) did not produce much differences between the steps. However, large steps (e.g *p*=1/2*)* may allow unseen regions to go missing during the process as the step size would be large.

By truncating 1/3 off the second peak of the histogram (i.e. *p*=1/3), part of the artifact managed to be reduced as shown in Fig. 5(c). The ROI remains unaffected with this threshold value but parts of the artifact remains. Hence, a further 1/3 step elimination (i.e. *p*=2/3) is carried on. Fig. 5(d) shows that a significant amount of the artifact has been successfully removed at this stage. The human brain can be more clearly identified now as compared to the original image.

Since there are still undesired spots of artifacts in the image, the whole second peak is removed. Referring to Fig. 5(e), it is now proven that almost all the visible area of the unwanted region has now been successfully removed. The important brain areas such as ventricle, diseased region and brain tissue are unaffected. The processed image is now more similar to the conventional MRI images, where the difference between the brain and the background can be distinguished clearly. The background and artifact have been completely removed and will no longer influence any consequent processing techniques applied to the image.

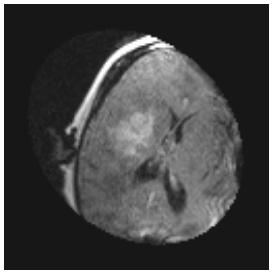

0 126 255

(a) Original image

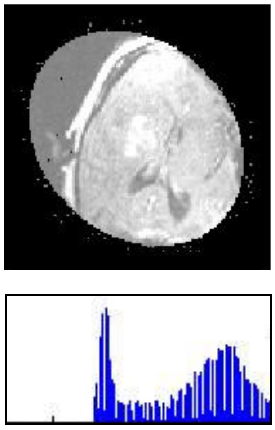

0 128 255

(b) P1 eliminated

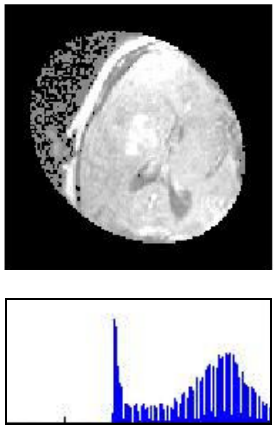

0 142 255

(c) 1/3 of P2 eliminated

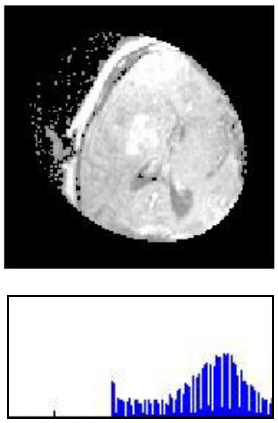

0 156 255

(d) 2/3 of P2 eliminated

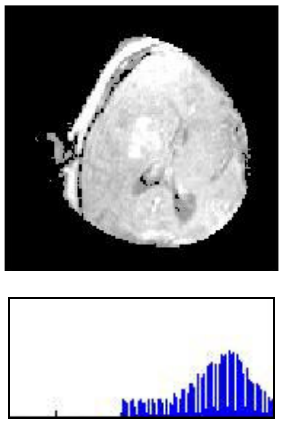

0 170 255

(e) Entire P2 eliminated

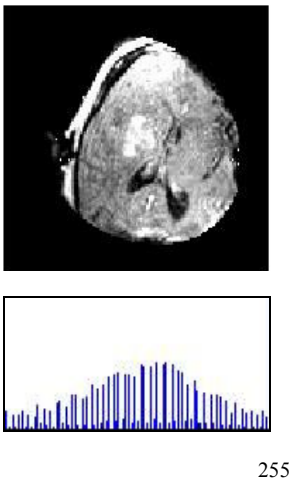

0 255

(f) Normalized image

Fig. 5. Histogram truncation and normalization

B. Normalization

Truncating the histogram peaks alone is not sufficient. Examining the images available, it was observed that the intensity range of the low-field MRI images are inconsistent (some in the higher ranges whilst others in the lower ranges). Thus, image normalization should be applied to the pre-processed image to standardize the intensity range to 0-255. By stretching the histogram, the image brightness will be more uniform. Some parts of the brain that were not clearly visible would become more obvious after normalization. Eq. (2) is used to normalize the image,

$$\text{Normalized image, } I = \frac{I_T - T}{max(I_T) - T} \times (2^{Cd} - 1) \qquad (2)$$

where I_T is thresholded image using threshold T, $max(I_T)$ is maximum intensity of I_T, Cd is the color depth (in bpp), e.g. $Cd = 8$ sets the grayscale intensity range between 0-255.

Fig. 5(f) shows the resulting histogram of the pre-processed image in Fig. 5(e), stretched from the range 155-255 to 0-255. A clearer image is produced and hence leads towards better identification of the ROI. As an example to illustrate the enhancement, notice that it is difficult to determine the boundaries of the bleed area in Fig. 5(e) (the white area near the middle of the brain). After the image is normalized, the differences can be seen clearly, without the application of any further complicated enhancement techniques. This reduces the time and cost of processing at the subsequent stages.

IV. Performance Assessment

To validate the performance of the proposed pre-processing technique, tests were conducted on the entire database. The results achieved by applying the proposed technique on a set of images with different characteristics are given below. The characteristics were chosen to compare the accuracy and robustness of the technique. The assessment performed encompasses both qualitative and quantitative measurements.

For the assessment, there are a number of criteria that need to be fulfilled in order to determine the effectiveness and consistency of the proposed method, in terms of the visibility of the pre-processed image, i.e. clear detail of the brain tissue, the existence of three main parts of the brain (skull, ventricle and brain tissue), as well as a complete elimination of non-brain area.

A. Visual Comparison

For the basic human visual evaluation, the test was divided into two categories – normal brain images and brain images with various diseases/ injuries. The results obtained are given in Fig. 6 and Fig. 7, respectively.

a) Normal Brain

For all 6 test images of patients with normal brain condition shown in Fig. 6, the separation between ventricle and white matter becomes more obvious after pre-processing. The same goes for the visibility of brain folds (consisting of gray matter). The artifacts in the original images were also successfully removed.

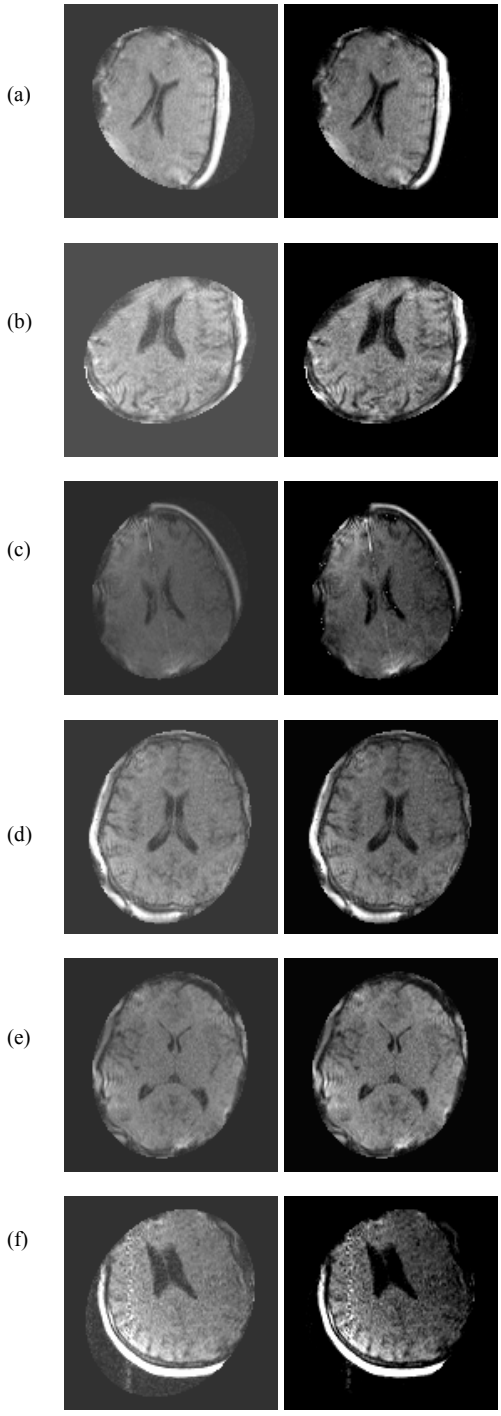

Fig. 6. Results of the proposed pre-processing technique on normal brain

In Fig. 6 (b), (d) and (e), it is obvious that all the details in the pre-processed image are visible enough for diagnosis, should there be any diseases. Besides, the properties of the images themselves, such as orientation, brain coverage and the clarity of the three main parts of the brain, makes it easier to evaluate these images.

For the results shown in Fig. 6 (a), (c) and (f), the orientation of the brain is tilted to the left or right in the different images. Despite the criteria stated before, the technique still produces excellent pre-processed image output. With this, it proves that the performance of the proposed method is excellent for normal low-field brain MRI images.

b) Diseased Brain

The image database obtained included a number of images that have been diagnosed with various diseases and injuries, such as bleeding, cyst, tumor, skull fracture, abnormalities as well as hydrocephalus of the ventricle. In addition, post-operation images are also included in this test.

Evaluating all of the images in Fig. 7, approximately 98% of the artifacts surrounding the brain ROI has been eliminated, regardless of the orientation of the brain. The output image is sharper than the original image without the need for further image sharpening. The details of the brain tissues are more prominent after the normalization.

Fig. 7(a) is an example of bleeding at the brain tissue boundaries. As can be seen in the original image, the separation between skull and bleeding area is less defined. However, after applying the pre-processing technique, a clear brain image with well-shaped boundaries between the brain tissues, bleeding as well as the skull is obtained.

Fig. 7(b) and (c) show more examples of bleeding in the brain. After image normalization, the brain folds become more visible. This can lead to a more precise segmentation with less distortion and noise. Fig. 7(d) shows ventricle abnormalities where in the original image, it is difficult to determine the brain folds and the actual brain ROI. The normalized brain image after the pre-processing phase can be seen clearly as compared to the original image.

Fig. 7(e) is a post-operation image where the skull has been separated. Fig. 7(f) is the post-operation brain image for Fig. 7(c). In both cases, the proposed technique has proven to be successful. In Fig. 7(g) – (k), the images comprise of various types of brain lesions. Due to the low resolution of the original images, it is difficult to distinguish the exact boundaries for all the tumors from the brain tissue as the intensity tends to be similar.

However, after truncating the unnecessary background artifact and normalizing the images, an obvious range of intensity can be observed especially at the boundaries between the tumors and brain tissue. This step is essential in order to accurately segment the diseased region for diagnosis As low-field MRI is used in the operating room to allow real-time imaging, such pre-processing would assist the surgeon in clearly distinguish the areas of interest.

The final image seen in Fig. 7(l) is that of a brain associated with a type of Alzheimer's disease called hydrocephalus. However, there is an unknown object detected during the scan. This type of additional artifact is not removed using the proposed technique as the object and its intended purpose is not known. As the object may have been deliberately included, or may be a vital part in aiding diagnosis, the output achieved as desired. Since the original image is rather dark, the histogram was almost equally distributed. There were no obvious peaks in this low quality image.

By observing all of the images in Fig. 7, the white marked arrow clearly shows the interested area to be eliminated since some of the image contrast unable to show the artifact boundaries. This proves the existence of elliptical shape aperture during the scanning using the low-field MRI machine. Thus, the actual brain image does not necessarily covered in all of the elliptical shape. The medical experts will only scan the area of interest for the surgery, such as tumor or bleeding area.

B. Additional Information

An alternative approach after the truncation of P1 is for the resulting histogram to be shifted to the left (see Fig. 8(a)). However, as the image becomes dimmer, the artifact is no longer visually obvious although it is still present and affects subsequent processing. Nonetheless, the same final result is obtained once the whole of P2 is removed. As such, either approach may be used.

In addition, to determine the amount of ROI that has been removed, subtracting the original image with the pre-processed image of Fig. 5(d) shows the differences as in Fig. 8(b). As observed, the whole background was eliminated and only very small parts of the brain area (see the few pixels in the brain area in the figure) were affected. This shows that the proposed technique is effective in eliminating unwanted regions while preserving the integrity of the areas of importance (i.e. the brain). The information provided by the image subtraction could be stored and used when further accuracy is required in subsequent processing.

C. Comparison of Edge Detection

Finding edges in an image is considered to be an important process in many artificial vision systems. There are three criteria that need to be fulfilled for optimal edge detection that will lead to better segmentation, namely, good localization, good detection as well as single response constraint which will return only one point for each true edge point. As an additional visual comparison to observe the differences between the original low-field MRI and the pre-processed image, Canny edge detection is applied.

Basically, the Canny edge detector [21] consists of four steps; smooth the image with a Gaussian filter, calculate the gradient of the smoothed image, apply non-maximal suppression, and perform hysteresis thresholding.

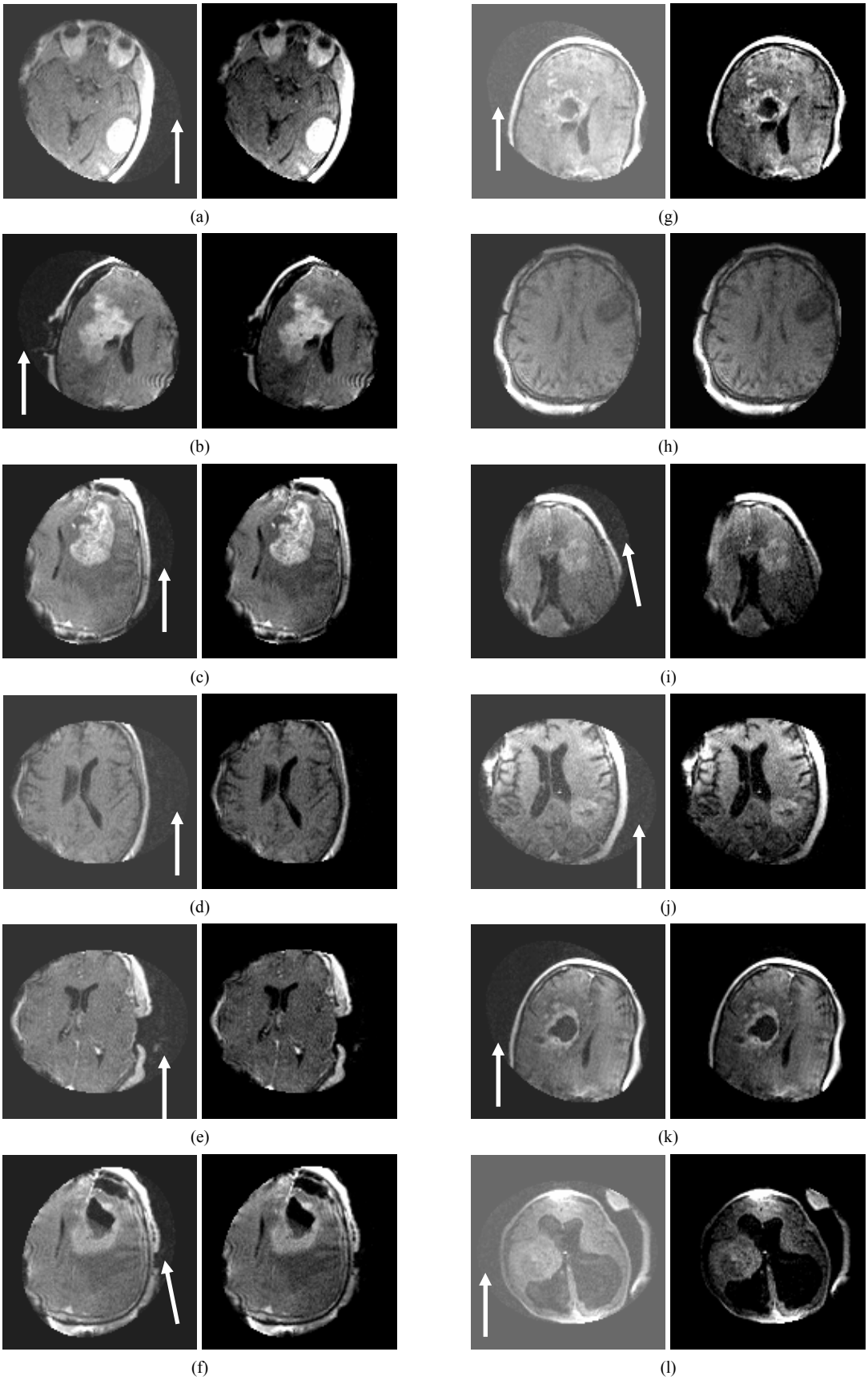

Fig. 7. Results of the proposed pre-processing technique on brain with diseases and injury

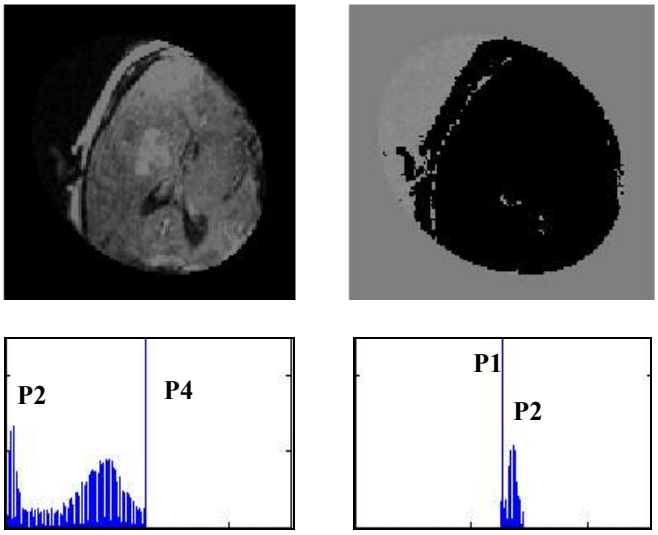

(a) Shifted histogram (b) Subtracted region

Fig. 8. Additional information for the alternative approach

A comparison of the selected edges for both original and pre-processed images can be seen in Fig. 9. A threshold value of 0.02 was applied to reduce the number of false edges since higher threshold value will cause some edges to disappear. From the results, it is shown that the pre-processed image eliminates false edges caused by the artifacts. Furthermore, the actual brain boundaries can be determined easily compared to the original edges.

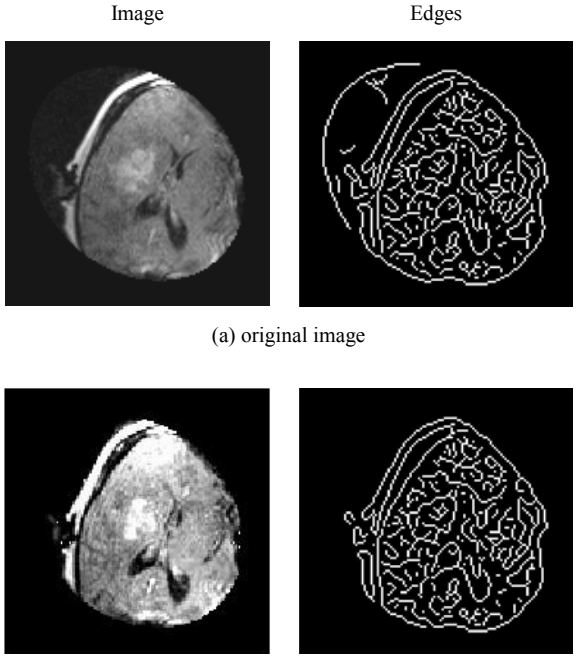

(a) original image

(b) pre-processed image

Fig. 9. Results using Canny edge detector

Using a larger set of images from various slices, the results in Fig. 10 show that the artifact in the original images is detected by using Canny edge detector (marked with the arrow), but the pre-processed images effectively eliminated almost all traces of the artifact. Only three of the images shown (Fig. 10 (d, f, g(iv))) detected a small pixels which could not be removed due to the unrecognized artifacts existed in the original image.

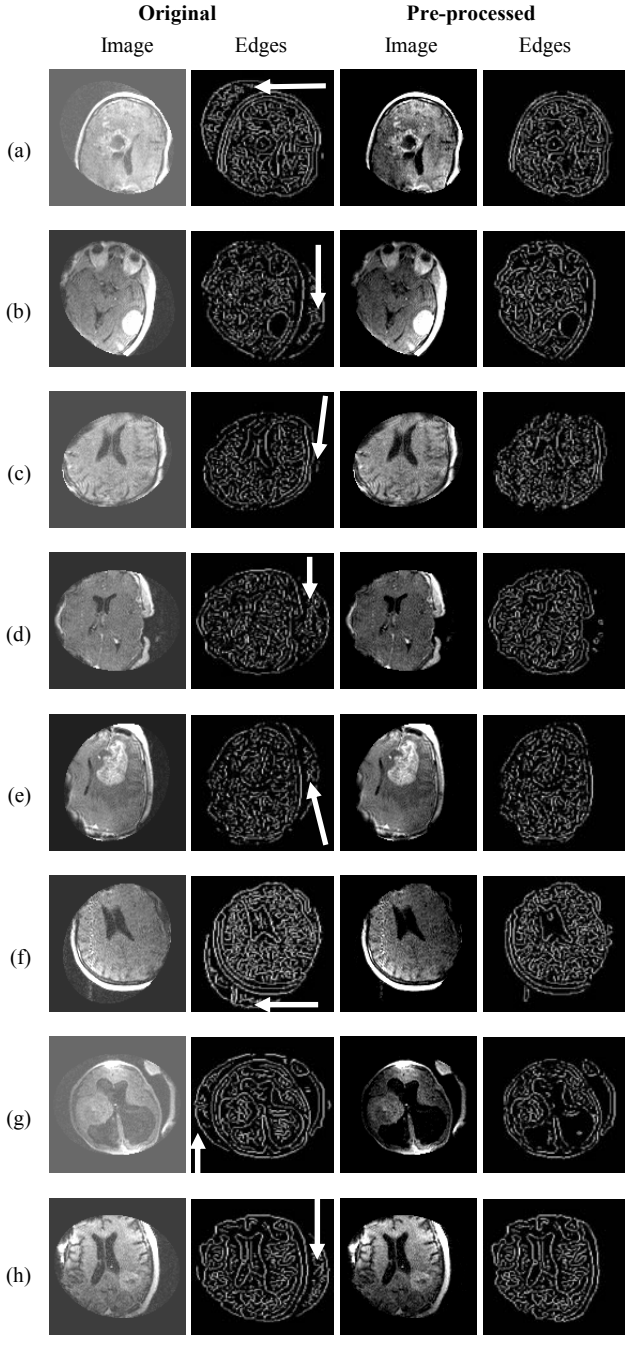

Fig. 10. Comparison of original and pre-processed images using Canny edge detector

D. Entropy

The effect of the proposed pre-processing technique can also be quantified by measuring the image's entropy, which is the amount of its information content. Image data entropy can be estimated from a gray level histogram. The entropy is defined by (3).

$$\text{Entropy} = -\sum_i P_i \, Log_2 P_i \tag{3}$$

where P_i is the probability that the difference between two adjacent pixels is equal to i, and Log_2 is the base 2 logarithm.

According to [22], a relatively complex image has higher entropy than a relatively simple image. As an example, an image that is perfectly flat will have an entropy of zero while high entropy images such as an image of heavily cratered areas on the moon have a great deal of contrast from one pixel to the next.

In Table 1 and 2, the entropy of the original and normalized pre-processed images is shown for normal brain images (Fig. 6) and diseased brain images (Fig. 7), respectively. As stated previously, the entropy is higher for complex images, as compared to simple ones. In this case, the original image is more complex image due to the texture caused by the noise. Hence, the entropy should decrease as the image is normalized.

TABLE 1: ENTROPY FOR NORMAL BRAIN

IMAGES (FIG. 6)	ORIGINAL	NORMALIZED
(a)	3.7564	3.3220
(b)	3.6214	3.6107
(c)	3.9211	3.4492
(d)	4.1783	4.1783
(e)	3.8138	3.8138
(f)	4.4469	3.5379

TABLE 2: ENTROPY FOR DISEASED BRAIN

IMAGES (FIG. 7)	ORIGINAL	NORMALIZED
(a)	4.4329	3.6600
(b)	4.2075	3.0363
(c)	4.4215	3.4455
(d)	4.2535	4.2535
(e)	4.3713	3.8561
(f)	3.7961	2.9920
(g)	4.1707	3.4132
(h)	4.5571	3.8577
(i)	4.2039	3.4218
(j)	4.3762	3.5560
(k)	4.4725	4.0331
(l)	4.1644	2.4366

From the results in Table 1 for normal brain images, it can be seen that the entropy for most of the normalized images is less than those of the original images. However, for Fig. 6(d) and (e), there was no difference due to the minimum existence of artifact in the original images.

By referring to Table 2 which consists of various brain diseases, it is observed that the same results were achieved as well. There is only one image (Fig. 7(d)) where there was no obvious artifact in the original image.

All the results above prove the effectiveness of the proposed scheme in clearing up the low-field brain MRI images. The normalized pre-processed images are not only visually improved, they are also more accurate for the purposes of segmentation and other computer-aided tasks.

V. CONCLUSION

Low-field MRI is now being introduced in medical institutions for real-time imaging during brain surgeries. However, the low signal strength produces low-resolution images and leads to difficulty in automated techniques.

This work proposes a dynamic thresholding and image normalization technique for enhancement of low-field brain MRI images. By controlled truncating and normalizing the histogram, the scheme eliminates the unnecessary background noise and artifacts in the image. The clarity of the ROI was enhanced effectively while almost no loss of information or image integrity was recorded in the actual brain areas of the processed low-field MRI images.

It is shown in this paper that in the histogram of a typical low-field MRI image, the first peak tends to be the image background, with the second peak being the acquisition artifact. The part of concern is the intensity around the third peak, which consists of the main brain regions.

As qualitative visual human observation may be subjective, quantitative measurement has also been taken into account to evaluate the differences between the original and pre-processed images. Out of entire database tested, minor inaccuracy (1 for normal and 2 for diseased) have been detected. Thus, the results show that more than 85% of the test images performed as expected in eliminating all non-ROI parts.

In future, further evaluation on special cases, such as the existing of non-removable artifacts of the histogram will be undertaken. The finalized image normalization technique could be used directly for feature extraction and segmentation. However, it is recommended that after pre-processing the image, denoising filters should be applied to remove any residue noise that may still present in the image, as proposed in [23]. The efficiency, robustness and accuracy of the pre-processing performance could be improved with further detailed analysis.

ACKNOWLEDGMENT

The authors would like to thank the Department of Neurosurgery, Maastricht University Hospital and the Department of Biomedical Engineering, Eindhoven University of Technology (TU/e), for providing the low-field MRI images used in this study. This project was supported by the Ministry of Science, Technology and Innovation (MOSTI), Malaysia through the Science Fund grant.

REFERENCES

[1] F. Ségonne, A.M. Dale, E. Busa, M. Glessner, D. Salat, H.K. Hahn, B. Fischl, "A hybrid approach to the skull stripping problem in MRI," *NeuroImage*, vol. 22, pp. 1060-1075, 2004.

[2] I.V. Gribkov, P.P Koltsov, N.V. Kotovich, A.A. Kravchenko, A.S. Koutsaev, A.S. Osipov, A.V. Zakharov, "Testing of image segmentation methods", *WSEAS Trans on Signal Processing*, Vol. 7, 2008.

[3] K. Rehm, "Medical Image Segmentation," *Lecture Notes on Advance Digital Imaging Science,* University of Minnesota, 2002.

[4] J. Rexilius, H.K. Hahn, J. Klein, M.G. Lentschig, H.O. Peitgen, "Multispectral brain tumor segmentation based on histogram model adaptation," *Proceedings of SPIE Conference on Medical Image Computing*, vol. 4, pp. 65140V-1-65140V-10, 2007.

[5] U. Vovk, F. Pernu, B. Likar, "Simultaneous correlation of intensity inhomogeneity in multichannel MR images," *27th Annual Conf. Engineering in Medicine and Biology,* pp. 4290-4293, 2005.

[6] N.I. Weisenfeld, S.K. Warfield, "Normalization of joint image-intensity statistics in MRI using the Kullback-Leibler divergence," *IEEE Symposium on Biomedical Imaging : Nano to Macro*, vol. 1, pp. 101-104, 2004.

[7] A. Madabhushi, J.K. Udupa, "Interplay between intensity standardization and inhomogeneity correction in MR image processing," *IEEE Trans. on Medical Imaging*, vol. 24, pp. 561-576, 2005.

[8] U. Vovk, F. Pernus, B. Likar, "A review of methods for correction of intensity inhomogeneity in MRI," *IEEE Trans. on Medical Imaging*, vol. 26, pp. 405-421, 2007.

[9] Y.L. Liao, N.T. Chiu, C.M. Weng, Y.N. Sun, "Registration and normalization techniques for assessing brain functional images," *Biomedical Engineering Applications, Basis & Communications*, 2003.

[10] J.G. Park, T. Jeong, C. Lee, "Automated brain segmentation algorithm for 3D magnetic resonance brain images," *2nd Intl. Workshop on Soft Computing Applications (SOFA)*, pp. 57-61, 2007.

[11] Y. Zhengmao, M. Habib, Y. Yongmau, "Digital trimulus color image enhancing and quantitative information measuring," *6th WSEAS Intl. Conf. on Information Security and Privacy,* pp. 323-328, 2007.

[12] N.F. Ishak, M.J. Gangeh, and R. Logeswaran, "A preliminary study of high-field MRI image enhancement techniques applied to low-field MR brain images," *4th Intl. Conf. on Biomedical Engineering (BIOMED),* vol. 21, pp. 482-486, 2008.

[13] M. Ballan, F. Gurgen, "Gradient based fingerprint verification using principal components," *IEEE Advances in Intelligence Systems and Computer Design (IMACS),* pp. 191 – 196, 1999.

[14] A.S. Rosalina, S.K. Tan, A.R. Nuraini, "Live-cell image enhancement using center weighted median filter," *11th WSEAS Intl. Conf. on Computers,* pp. 382-385, 2007.

[15] H.A. Ali, B.M. Ne'ma, "Multi-purpose code generation using fingerprint images", *6th WSEAS Intl. Conf. on Information Security and Privacy,* pp. 141-145, 2007.

[16] N. Savage, "A weaker, cheaper MRI," *IEEE Spectrum*, vol. 45, no. 1, pp. 21, January 2008.

[17] P. Hastreiter, C.R. Salama, G. Soza, M. Baeur, et. al, "Strategies for brain shift evaluation," *Medical Image Analysis*, vol. 8, pp. 447-464, 2004.

[18] T. Magee, M. Shapiro, and D. Williams, "Comparison of high-field-strength versus low-field-strength MRI of the shoulder," *American Journal of Roentgenology,* pp. 1211-1215, 2003.

[19] M.B. Ahmad, and T.S. Choi, "Local threshold and Boolean function based edge detection," *IEEE Trans. On Consumer Electronics*, vol. 45, pp. 332-333, 1999.

[20] C.S. Yung, S.H. Ki, M.N. Seung, and W.P. Jong, "Threshold estimation for region segmentation of MR image of brain having the partial volume artifact," *5th Intl. Conf. on Signal Processing Proceedings (ICSP),* vol. 2, pp. 1000-1009, 2000.

[21] J.F. Canny, "A computational approach to edge detection." *IEEE Trans. On Pattern Analysis and Machine Intelligence (PAMI),* vol. 8, pp. 679-698, 1986.

[22] Y. Zhengmao, M. Habib, Y. Yongmau, "Image contrast enhancement and quantitative measuring of information flow," *6th WSEAS Intl. Conf. on Information Security and Privacy,* pp. 172-177, 2007.

[23] N.F. Ishak, M.J. Gangeh, and R. Logeswaran, "Comparison of denoising techniques applied on low-field MR brain images," *5th Intl. Conf. on Computer Graphics, Imaging and Visualization (CGIV),* pp. 345–349, 2008.

Nur Faiza Ishak was born in Kuala Lumpur, Malaysia on the February 08th, 1984. She received the B. Eng. (Hons) degree in Electronics (majoring in Telecommunications) from the Faculty of Engineering and Technology, Multimedia University, Melaka, Malaysia in 2007.

She is currently a Research Officer at the Faculty of Engineering, Multimedia University, Cyberjaya, Selangor, Malaysia. Her research areas are in image processing, low-field MRI and brain segmentation.

Rajasvaran Logeswaran received his B. Eng. (Hons) Computing degree from the University of London (Imperial College of Science, Technology and Medicine), United Kingdom in 1997, M.Eng.Sc. and Ph.D. degrees from Multimedia University, Cyberjaya in 2000 and 2006, respectively.

He was an Assistant Professor at The Global School of Media, Soongsil University, South Korea in 2008. He is currently a Senior Lecturer at the Faculty of Engineering, Multimedia University, Cyberjaya, Malaysia. His research interests comprises of neural network, data compression, medical image processing and web technology.

Tan Wooi Haw received his M. Sc. (Electronics) from Queen's University of Belfast in 1998. His research interest is in image processing and analysis, as well as swarm intelligence. He is a Lecturer at the Faculty of Engineering, Multimedia University, Cyberjaya, Malaysia.